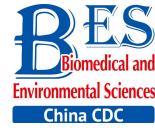


Original Article



Increased PIT1 and PIT2 Expression in Streptozotocin (STZ)-induced Diabetic Mice Contributes to Uptake of iAs^V *

YU Sha Li^{1,^}, XU Ling Fei^{1,^}, WU Jun Xia^{1,^}, YAO Chen Juan², HU Qiao Yun¹, ZHANG Chun Xue¹, ZHAO Xin Yuan¹, WEI Hai Yan¹, WANG Xiao Ke^{1,#}, and CHEN Gang^{1,#}

1. Department of Environmental Health, School of Public Health, Nantong University, Nantong 226019, Jiangsu, China; 2. Department of Molecular Oral Physiology, Institute of Biomedical Sciences, Tokushima University Graduate School, 770-8504, Japan

Abstract

Objective This study aimed to investigate the susceptibility of mice with streptozotocin(STZ)-induced diabetes mellitus (T1DM) to the uptake of pentavalent inorganic arsenic (iAs^V) and the possible molecular mechanism.

Methods T1DM was induced in mice by STZ. T1DM and normal mice were treated with 15.0 mg/kg $Na_2HAsO_4 \cdot 12H_2O$ by intragastric administration. Then, the concentrations of arsenic in various tissues were measured by atomic fluorescence spectrometry. The gene expression levels of *Pit1* and *Pit2* were quantified by real-time RT-PCR, and their protein levels were detected by Western blotting in mouse heart, kidney, and liver tissues.

Results The concentrations of arsenic in STZ-induced T1DM mouse tissues were higher at 2 h after intragastric administration of $Na_2HAsO_4 \cdot 12H_2O$. Compared with the levels in normal mice, PIT1 and PIT2, which play a role in the uptake of iAs^V , were upregulated in the livers and hearts of T1DM mice. PIT1 but not PIT2 was higher in T1DM mouse kidneys. The upregulation of *Pit1* and *Pit2* expression could be reversed by insulin treatment.

Conclusion The increased uptake of iAs^V in T1DM mouse tissues may be associated with increased PIT1 and/or PIT2 expression.

Key words: Type I diabetes mellitus; Pentavalent inorganic arsenic; Uptake; Phosphate cotransporters

Biomed Environ Sci, 2017; 30(11): 792-801

doi: 10.3967/bes2017.107

ISSN: 0895-3988

www.besjournal.com (full text)

CN: 11-2816/Q

Copyright ©2017 by China CDC

INTRODUCTION

Arsenic, one of the most ubiquitous toxins, is widely distributed in soil and water and endangers the health of humans

worldwide^[1]. Inorganic arsenic has a wide range of adverse health effects, including skin lesions^[2], cardiovascular diseases^[3], diabetes^[4], birth defects^[5], abortion^[6], cognitive impairment^[7], and cancer^[8]. Arsenic exists in trivalent arsenic (As^{III}) and

*This study was supported by the National Natural Science Foundation of China [grant numbers 21277078, 21407082]; the Natural Science Foundation of Jiangsu Province [grant numbers BK20140426]; the Natural Science Fund Project of Colleges in Jiangsu Province [grant numbers 16KJB330007]; and the National Undergraduate Innovation Experiment Project [grant numbers 201510304037Z].

[^]These authors contributed equally to this work.

[#]Correspondence should be addressed to CHEN Gang, WANG Xiao Ke, Tel: 86-513-85012912, Fax: 86-513-85012900, E-mail: chengang@ntu.edu.cn; wxke111@hotmail.com

Biographical notes of the first authors: YU Sha Li, female, born in 1983, PhD, lecturer, majoring in environmental toxicology; XU Ling Fei, male, born in 1989, MPH, majoring in public health and molecular biology; WU Jun Xia, female, born in 1986, MPH, majoring in public health and molecular biology.

pentavalent arsenic ($iAs^{(V)}$) forms. Based on the molecular similarities between arsenate and phosphate, it has generally been assumed that $iAs^{(V)}$ enters mammalian cells *via* inorganic phosphate (Pi) transporters^[9]. Pi transporters are known to catalyze the uptake of Pi across the plasma membrane in mammalian cells^[10-11]. They are grouped into three families, namely type I-III sodium/phosphate cotransporters^[11-12]. Type I (SLC17 family) cotransporters are involved in organic anion transport, including that of phosphate, while their role in Pi homeostasis is unclear^[13]. Type II sodium/phosphate cotransporters (SLC34 family) are expressed in a tissue-specific manner: NaPi-IIa and NaPi-IIc are mainly expressed in the kidney^[14], and NaPi-IIb is expressed in the intestines, lung, testis, and kidney^[15]. Type III (SLC20 family, PIT1, and PIT2) cotransporters, which are expressed ubiquitously in all tissues, have been proposed to function in general transport of Pi into cells and have been identified as the predominant phosphate transporters in rats^[16]. Several studies have shown that arsenate is a substrate for members of the SLC34 and SLC20 family of Na^+ -Pi cotransporters^[17-20].

Diabetes mellitus, a chronic metabolic disease, has become one of the most prevalent non-communicable diseases worldwide. Diabetes mellitus is divided into two types, type I and type II. Type I diabetes mellitus (T1DM) is a disorder that arises following the autoimmune destruction of insulin-producing pancreatic β cells^[21-22], which usually presents as a classic trio of symptoms (polydipsia, polyphagia, and polyuria) alongside overt hyperglycemia^[23]. T1DM has various adverse impacts on many tissues, such as the kidney, heart, retina, liver, lung, vasculature, and skeletal muscle^[24]. Many gene expression levels are altered in the liver and lungs of T1DM rats^[25-26], which might contribute to the increased susceptibility to toxins associated with diabetes. For example, STZ-induced T1DM rats are more susceptible to cadmium nephrotoxicity than are normal rats^[27].

In this study, arsenic was found to be absorbed to a greater extent in many different tissues of T1DM mice than in the tissues of normal mice at 2 h after treatment with 15.0 mg/kg pentavalent arsenic ($Na_2HAsO_4 \cdot 12H_2O$). To explore the possible molecular mechanism underlying this increased uptake of arsenate in diabetic animals, sodium/phosphate cotransporters were studied. Type II sodium/phosphate cotransporters have

tissue-specific expression, while type III sodium/phosphate cotransporters are widely expressed in most tissues. Therefore, the type III sodium/phosphate cotransporters PIT1 and PIT2 were chosen for this study. To determine whether altered PIT1 and PIT2 expression was associated with genetic upregulation, their expression levels were evaluated in the heart, kidneys, and liver, the chief arsenic target organs, along with the effect of insulin treatment in T1DM mice induced by STZ.

MATERIALS AND METHODS

Animals and Treatments

Male ICR mice were obtained from the Experimental Animal Center of Nantong University, China. They were maintained in a specific-pathogen-free barrier facility under a reverse 12-h light/dark cycle (lights off at 10:00 am) and acclimatized for 3 days before the experiments. The use of animals for this study was approved by the institutional animal ethics committee of Nantong University.

Sixty mice, weighing 20-24 g, were divided into 10 groups, then 9 groups were treated with 15.0 mg/kg $Na_2HAsO_4 \cdot 12H_2O$ (Chengdu boruite chemical technology Co., Ltd, Chengdu, China) by intragastric administration after 5 h of fasting (with free access to water). Six mice in each group were euthanized at 0, 0.5, 1, 2, 3, 6, 12, 24, and 48 h after treatment, and tissue samples were removed and stored in a deep freezer at $-80^\circ C$ for the measurement of arsenic. The last six mice were treated with saline and used as the control group. Tissues of mice in the control and 2 h post-exposure groups were removed for detection of mRNA expression of *Pit1* and *Pit2*.

To prepare the STZ-induced diabetic mouse model, 24 mice, weighing 17-19 g, were fasted for 12 h with free access to water, and then fasting blood glucose levels was determined in blood samples obtained from the tail vein. Mice were then randomly divided into two groups, namely the T1DM group ($n = 13$) and the normal group ($n = 11$). The T1DM group was intraperitoneally (i.p.) injected with STZ (Sigma-Aldrich, Co. St. Louis, MO, USA) dissolved in citric acid-sodium citrate buffer (pH 4.4) at a dose of 60.0 mg/(kg-bw), whereas the normal group was injected with the same amount of the vehicle solution. STZ and vehicle solution were injected once per day for 5 consecutive days. The mice were

monitored for 12 days following the last injection. Body weights and food and water intake were recorded every day. Fasting blood glucose levels were measured on the last day.

The mice in the T1DM group with blood glucose concentrations greater than 11.1 mmol/L were considered to be STZ-induced stable diabetic mice^[28]. According to this criterion, two mice in the T1DM group were eliminated because their fasting blood glucose levels were less than 11.1 mmol/L. Then, 11 mice from each of the normal and T1DM groups were treated with 15.0 mg/kg Na₂HAsO₄·12H₂O by intragastric administration following fasting for 5 h (with free access to water). The mice were euthanized at 2 h after treatment, and tissues were removed and stored in a deep freezer at -80 °C for the measurement of arsenic levels.

To determine the mechanisms that modulate the expression of Na/Pi transporters, an insulin-treated group was also utilized. Eighteen mice, weighing 17-19 g, were split into three groups of six individuals: a normal group (Control), a diabetic group (T1DM), and a diabetic group treated with insulin (T1DMI). One day after confirmation of diabetes, the animals from the T1DMI group received daily subcutaneous injections of porcine pancreatic insulin [I113907-10 mg, 28.3 UPS units/mg (HPLC), Aladdin, China] diluted in 0.9% NaCl (5 IU twice a day, at 9 am and 9 pm). The animals in the normal and T1DM groups received saline injections by the same route during the study. The insulin doses were standardized under the same conditions used in the pilot study. The standardization was performed over a period of 14 days, and the protocol was chosen after careful evaluation of the glucose concentrations, which were measured throughout the day. The twice-daily 5-IU insulin dose outlined in the protocol had no impact on animal mortality, allowed better maintenance of glucose concentrations, and showed results similar to those of the control group. To avoid the influence of changes in blood glucose, all mice were injected with insulin at 9 am, and tissues were collected between 10 am and 12 pm to detect *Pit1* and *Pit2* mRNA. The PIT1 and PIT2 protein levels were detected in normal and diabetic mouse tissues. Before sacrifice, the fasting blood glucose levels of T1DMI mice were all measured to be less than 6.0 mmol/L.

Measurement of Fasting Blood Glucose

The fasting blood glucose levels were measured using an Accu-Chek Advantage glucometer (Roche

Diagnostics GmbH, Mannheim, Germany).

Measurement of Arsenic in Mouse Tissues

Briefly, an approximately 200.0 mg tissue sample was placed in a beaker, mixed with 5.0 mL of ultrapure concentrated HNO₃ (Sinopharm chemical reagent Co., Ltd, Shanghai, China), and then incubated at room temperature overnight. Next, the beaker was placed on a hot plate at 90-100 °C. Then, approximately 6.0 mL of a freshly prepared mixture of concentrated HNO₃ and H₂O₂ (1:1, v/v) was added to each beaker and heated to 100 °C after hydrolysis of concentrated HNO₃. After drying, 3.0 mL of 30% H₂O₂ was added and further heated until the solution became colorless. Following hydrolysis, all materials in the beaker were transferred to a 15.0 mL test tube. The residue in the beakers was then thoroughly washed with distilled water and combined with the hydrolysate described above. The final volume of the mixture was exactly 9.0 mL. Finally, 0.5 mL of 150 g/L thiourea solution and 0.5 mL of 36% concentrated hydrochloric acid were added to each tube. The concentration of arsenic was measured with an atomic fluorescence spectrometer AFS-9700 machine (Kchaiguang Instrument Co., Ltd. Beijing, China), using 5% hydrochloric acid as the carrier liquid, high-purity argon as the carrier gas, and potassium borohydride as the reducing agent.

Semi-quantitative PCR and Real-time Quantitative RT-PCR

Total RNA was extracted using an RNAiso™ Plus kit (TaKaRa Biotechnology Co., Ltd, Dalian, China) following the manufacturer's instructions. Single-stranded cDNA was synthesized from 3.5 µg of total RNA with an M-MLV reverse transcriptase kit (TaKaRa Biotechnology Co., Ltd, Dalian, China). For a visual evaluation of mRNA expression, routine RT-PCR was also performed. Hypoxanthine guanine phosphoribosyl transferase (*Hprt*) was used as the loading control for heart tissue, and *β-actin* was used as the control for liver and kidney tissues. The primer sequences are listed in Table 1. PCR was performed in a thermal cycler as follows: initial denaturation at 94 °C for 4 min; cycles of denaturation at 94 °C for 30 s, annealing at various temperatures (Table 1) for 30 s, and extension at 72 °C for 1 min; and a final 10 min extension at 72 °C (Bio-Rad Laboratories, Inc. Hercules, CA, USA).

PCR products (10 µL) were electrophoresed on a 1.5% agarose gel containing 0.5 µg/mL ethidium

bromide, and the gel was exposed to UV light and imaged with a Gel Doc™ XR Gel Documentation System (Bio-Rad Laboratories, Inc. Hercules, CA, USA).

The synthesized cDNA was also subjected to real-time PCR in a Light Cycler[®] 480 II (Roche Diagnostics GmbH, Mannheim, Germany) using SYBR enzyme (TaKaRa Biotechnology Co., Ltd, Dalian, China). The reaction mixture (5.0 µL of 2x SYBR enzyme, 0.4 µmol/L aliquots of sense and anti-sense primers, approximately 100 ng of cDNA, and ddH₂O up to a final reaction volume of 10 µL) was heated to 95 °C for 15 s, followed by 40 cycles of PCR consisting of annealing for 15 s and extension at 72 °C for 20 s. Melting curve analysis was used to confirm the purity of the PCR product. Data were analyzed using the 2^{-ΔΔCt} method.

Western Blotting

Mouse tissues were isolated using RIPA buffer (150 mmol/L NaCl, 1% TritonX-100, 50 mmol/L Tris pH 7.4, 1% sodium deoxycholate, 0.1% SDS, 1 mmol/L PMSF) supplemented with a protease inhibitor cocktail (Roche Diagnostics GmbH, Mannheim, Germany). Protein concentrations were determined by using a Bio-Rad protein assay kit (Bio-Rad Laboratories, Inc. Hercules, CA, USA) with bovine serum albumin as a standard. The proteins were mixed with 2x SDS sample buffer and denatured at 95 °C for 10 min. Equal amounts of protein samples were separated by SDS-PAGE. Separated proteins were electrophoretically transferred onto polyvinylidene fluoride membranes in a mini-protein II Electrophoresis Apparatus (Bio-Rad). The blotted

membrane was blocked with 0.1% TBST containing 3% nonfat dry milk at room temperature for 2 h and then incubated with the corresponding primary antibody at 4 °C overnight. The dilutions of anti-SLC20A1 antibody (ab177147, Abcam, Cambridge, MA, USA) and anti-SLC20A2 antibody (ab191182, Abcam, Cambridge, MA, USA) were both diluted to 1:1,000 in 0.1% TBST. As an internal standard, β-actin antibody (1:20,000) (A5316, Sigma-Aldrich, Co. St. Louis, MO, USA) (for the liver and kidneys) and rabbit antiglyceraldehyde-3-phosphate dehydrogenase (GAPDH) antibody (1:20,000) (G9545, Sigma-Aldrich, Co. St. Louis, MO, USA) (for the heart) were used. The membrane was washed with 0.1% TBST and incubated with goat anti-rabbit IgG-HRP (1:20,000) (BS13278, Bioworld Technology, Co., Ltd, Minneapolis, USA) at room temperature for 1 h, followed by another wash with 0.1% TBST. The membrane was then incubated with Immobilon™ Western Chemiluminescent HRP Substrate (Millipore Corporation, Billerica, MA, USA) and imaged with a Tanon-5200 system (Tanon Company, Shanghai, China). Densitometric analysis of each protein on the western blot was performed to quantify signal intensities using Image J software, with the loading control normalized to 1.

Statistical Analysis

At least five biological replicates were used for each analysis. All results are presented as the means ± standard deviations (mean ± SD), and data were analyzed statistically using SPSS17.0 software (SPSS Inc., USA). Results were considered statistically significant at $P < 0.05$ in the Student's *t*-test.

Table 1. Primers Used in Semi-quantitative PCR and Real-time Quantitative PCR

Genes		Primers (5'-3')	Tm (°C)	Cycles*	Size (bp)
Mouse- <i>Pit1</i> (XM-011239399)	sense	GAAGGAGGAGACCAGCATAG	55	23/27/24	245
	anti-sense	GAAGTGTAGCTGTTGTTGCG			
Mouse- <i>Pit2</i> (NM-011394)	sense	GAATCTCTACAACGAGACCG	56	24/27/24	199
	anti-sense	CAATCTTGACGAGCTCCATC			
<i>β-actin</i> (NM-007393)	sense	CTCCGGAGTCCATCACAATG	57	24/24/24	199
	anti-sense	CTACAATGAGCTGCGTGTGG			
<i>Hprt</i> (NM-013556)	sense	GACTTGCTCGAGATGTCATG	55	24/24/24	379
	anti-sense	GTATCCAACACTTCGAGAGG			

Note. * Cycle numbers applied for semi-quantitative PCR amplification of total RNA from the heart, liver, and kidney, respectively.

RESULTS

Time-dependent of Changes in Arsenic Levels in Mouse Tissues after Arsenate Administration

To examine the iAs^V uptake in mouse tissues, mice were given 15.0 mg/kg $Na_2HAsO_4 \cdot 12H_2O$ by intragastric administration. The concentrations of arsenic in five tissue types are shown in Figure 1. The peak concentration of arsenic in the liver, kidneys, heart, lungs, and testis was reached at 1, 0.5, 2, 3, and 6 h, respectively. Therefore, we compared iAs^V uptake in the normal and the TIDM groups at 2.0 h after arsenate treatment in this study.

Evaluation of STZ-induced TIDM Mice

The body weight, food intake and water intake of mice were measured every day when the STZ was injected. After STZ administration blood glucose levels were significantly increased in TIDM mice, and their body weights were notably reduced compared with the normal group (Table 2).

Increased Arsenic Concentration in TIDM Mouse Tissues

Both normal and TIDM mice underwent intragastric administration of 15.0 mg/kg $Na_2HAsO_4 \cdot 12H_2O$. Two hours after treatment, the mice were sacrificed, and the arsenic concentrations in various tissues were evaluated. The results showed that the arsenic levels were significantly increased in the liver, kidneys, heart, spleen, submandibular gland, testis, and brain tissues of TIDM mice compared with those of the

normal group. These results indicated that arsenate was absorbed to a greater extent in various tissues of TIDM mice (Table 3).

Increased Expression Levels of PIT1 and PIT2 in the Tissues of TIDM Mice, Reversed by Insulin Administration

To explore the mechanism involved in increased arsenate uptake in TIDM mice, we first examined whether iAs^V itself altered the expression of genes associated with arsenate uptake. Normal mice were treated with or without 15.0 mg/kg $Na_2HAsO_4 \cdot 12H_2O$

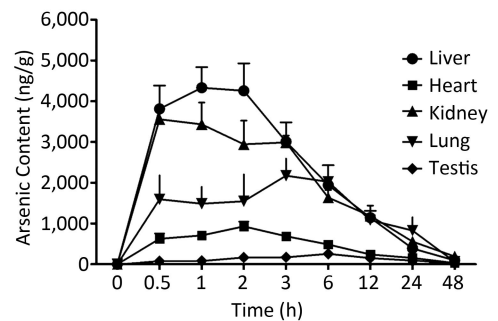


Figure 1. Arsenic concentrations in mouse tissues after intragastric administration of iAs^V . A total of 15.0 mg/kg $Na_2HAsO_4 \cdot 12H_2O$ was given once to mice by intragastric administration. The mice were sacrificed at the indicated time points after treatment with iAs^V . The arsenic concentration in each tissue type was measured by atomic fluorescence spectrometer. The values are shown as the means \pm SD, $n = 6$.

Table 2. Assessment of STZ-induced Diabetes Mellitus Mice

Mice	Baseline Body Weight (g)	Baseline Blood Glucose before (mmol/L)	Body Weight (g)	Blood Glucose After (mmol/L)
Control	17.15 \pm 0.82	5.88 \pm 0.96	31.29 \pm 3.83	5.93 \pm 1.15
TIDM	17.45 \pm 1.07	6.11 \pm 0.78	23.26 \pm 2.63**	21.34 \pm 2.42**

Note. Values are expressed as the means \pm SD, ($n = 16$). Control, normal mice with the vehicle solution. TIDM, diabetic mice induced by STZ. ** $P < 0.01$, significantly different from the respective control values.

Table 3. The Concentration of Arsenic in Various Tissues (ng/g)

Mice	Liver	Kidney	Lung	Heart	Spleen	Salivary Gland	Testis	Brain
Control	4266.47 \pm 1008.15	2945.00 \pm 844.92	1547.55 \pm 659.84	931.16 \pm 222.86	1922.09 \pm 520.20	581.95 \pm 193.00	155.05 \pm 49.37	129.32 \pm 48.88
TIDM	7884.62 \pm 1460.18**	3827.11 \pm 627.27*	2397.43 \pm 470.63**	1441.98 \pm 300.41**	2908.45 \pm 587.26**	973.79 \pm 281.41*	219.80 \pm 65.28*	200.91 \pm 73.52**

Note. Values are expressed as the means \pm SD, ($n = 11$). Control, normal mice with the vehicle solution; TIDM, diabetic mice induced by STZ. * $P < 0.05$, ** $P < 0.01$, significantly different from respective control values.

by intragastric administration, and the expression levels of *Pit1* and *Pit2* mRNA in the liver, kidney, and heart were examined 2 h after treatment. The results showed that neither *Pit1* nor *Pit2* gene expression levels were changed (Figure 2). These results suggested that the mRNA levels of *Pit1* and *Pit2* in those tissues were not affected by the treatment described above.

Next, we examined the *Pit1* and *Pit2* mRNA expression levels in the kidneys, hearts, and livers of normal, T1DM, and T1DMI mice. The *Pit1* mRNA expression level in the kidney tissue of T1DM mice was higher than that in the normal group but was downregulated in the T1DMI group, as determined by semi-quantitative RT-PCR (Figure 3A) and real-time quantitative RT-PCR (Figure 3B). Unlike that of *Pit1*, the expression level of *Pit2* mRNA was not changed in the T1DM and T1DMI groups (vs. Control, $P > 0.05$, Figure 3A-B). Similarly, PIT1 but not PIT2 protein levels in the kidney tissues of T1DM group mice were increased (vs. Control, $P < 0.05$, Figure 3C-D).

We next measured PIT1 and PIT2 expression in cardiac tissues. Compared with normal group mice, both *Pit1* and *Pit2* mRNA expression levels in the hearts of T1DM mice were increased, and this increase was reversed by insulin treatment in T1DMI mice, as shown by semi-quantitative RT-PCR and real-time quantitative RT-PCR (Figure 4A-B). Western blotting results further revealed that the PIT1 and PIT2 protein levels were increased in the hearts of T1DM mice (vs. Control, $P < 0.01$, Figure 4C-D). These results indicated that T1DM increased both PIT1 and PIT2 mRNA and protein expression levels in the hearts of mice.

Finally, we evaluated both PIT1 and PIT2 expression in the liver. Consistent with the results from cardiac tissues, PIT1 and PIT2 expression levels were higher in T1DM livers than in normal ones, and *Pit1* and *Pit2* mRNA expression was down-regulated by insulin treatment in T1DMI mice (Figure 5). Collectively, PIT1 and PIT2 expression was up-regulated in T1DM mice, which might account for the increased arsenic uptake.

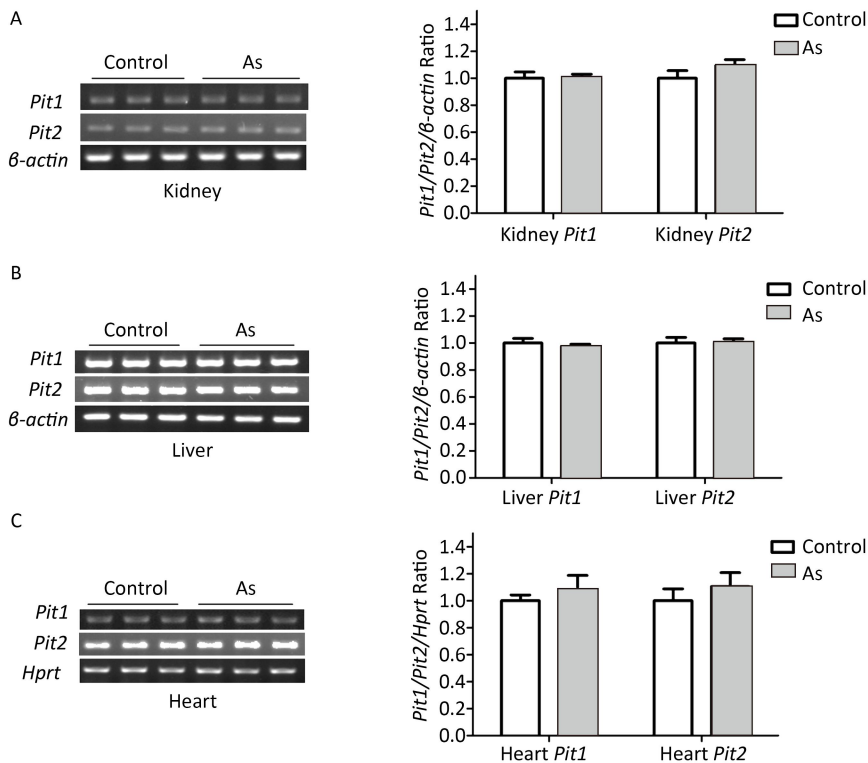


Figure 2. *Pit1* and *Pit2* mRNA expression levels in mouse tissues 2 h after exposure to arsenate. Representative semi-quantitative RT-PCR verifying mRNA expression levels of *Pit1* and *Pit2* in mouse kidney tissues (A), liver tissues (B), and cardiac tissues (C) before and after administration of $iAs^{(V)}$. Quantification shown to the right represents band intensity as measured with Quantity One image software. Control, mice that were treated with saline; As, mice that were treated with 15.0 mg/kg $Na_2HAsO_4 \cdot 12H_2O$. Data represent means \pm SD, $n = 6$.

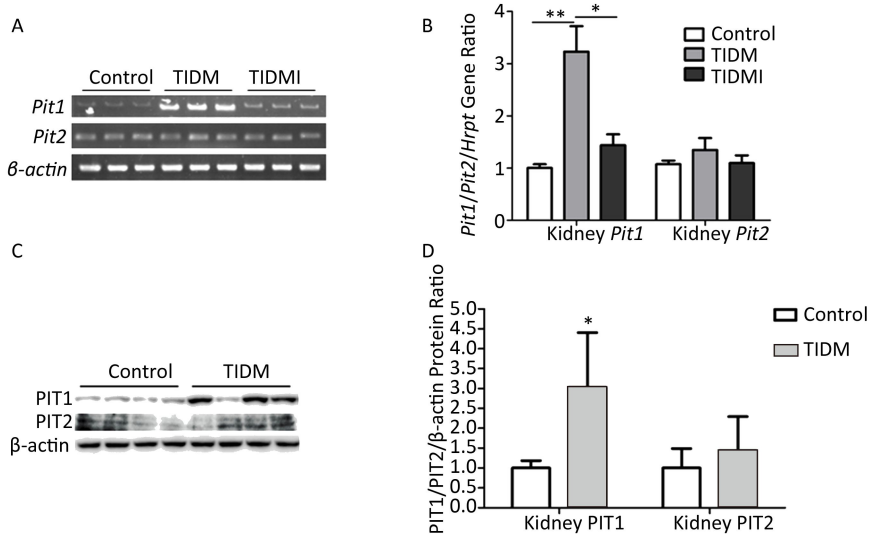


Figure 3. *Pit1*, *Pit2*, PIT1, and PIT2 expression levels in the kidneys of type I diabetic mellitus (T1DM) mice. (A) *Pit1* and *Pit2* mRNA expression levels were analyzed by semi-quantitative RT-PCR. (B) *Pit1* and *Pit2* mRNA expression levels were analyzed by real-time quantitative RT-PCR. (C-D) PIT1 and PIT2 protein expression levels in the kidney were determined by Western blotting. The band intensity of the blot was normalized to β -actin and quantified with Image J software. Data represent means \pm SD, $n = 6$. Control, normal mice; T1DM, diabetic mice induced by STZ; T1DMI, T1DM mice treated with insulin. * $P < 0.05$, ** $P < 0.01$.

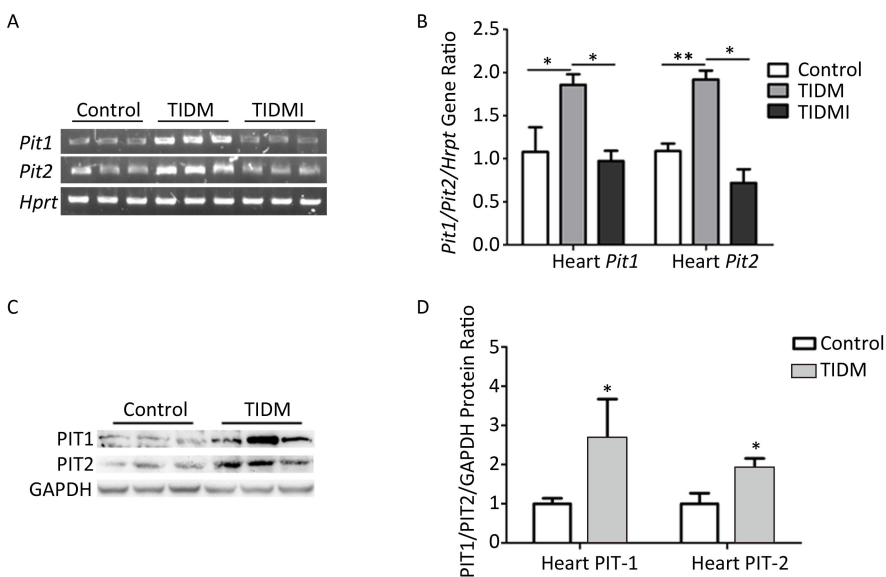


Figure 4. *Pit1*, *Pit2*, PIT1, and PIT2 expression levels in the hearts of type I diabetic mellitus (T1DM) mice. (A) *Pit1* and *Pit2* mRNA expression levels were analyzed by semi-quantitative RT-PCR. (B) *Pit1* and *Pit2* mRNA expression levels were analyzed by real-time quantitative RT-PCR. (C-D) PIT1 and PIT2 protein expression levels in the hearts were determined by Western blotting. The band intensity of the blot was normalized to GAPDH and quantified with Image J software. Data represent means \pm SD, $n = 6$. Control, normal mice; T1DM, diabetic mice induced by STZ; T1DMI, T1DM mice treated with insulin. * $P < 0.05$, ** $P < 0.01$.

DISCUSSION

In this study, it was found that STZ-induced T1DM mice were more susceptible to iAs^V uptake in various tissues than normal mice. The known efficient iAs^V transport systems include the type II and III sodium/phosphate cotransporters. Based on analysis of PIT1 and PIT2 expression and the effect of insulin on their modulations, the up-regulation of PIT1 and PIT2 in T1DM mice might contribute to the increased uptake of iAs^V in various tissues of these mice. To the best of our knowledge, this is an advanced report of increased iAs^V uptake in tissues of diabetes mellitus-afflicted animals. This indicates that higher expression of PIT1 and PIT2 may play an important role in increasing the transport of iAs^V into cells and tissues under diabetic conditions. Though the exact mechanism by which PIT1 and PIT2 expression is regulated in STZ-induced T1DM mice remains unclear, insulin deficiency has emerged as a potential mode of action. Insulin can regulate the expression of many genes that are involved in the control of metabolic processes associated with impaired glucose tolerance and diabetes^[29]. In our results, insulin reversed the up-regulation of *Pit1* and *Pit2* in T1DM mouse tissues. Therefore, defects in

insulin secretion could be at least partially associated with up-regulation of PIT1 and PIT2. Few studies of sodium/phosphate cotransporter expression induced by insulin *in vitro* have been published. Li et al. reported that the *NaPi-II* and *Pit2* genes were not regulated by insulin in primary rat hepatocyte cultures^[30]. However, insulin has been shown to stimulate *Pit1* mRNA and protein expression modestly in medial artery vascular smooth muscle cells^[31]. Our findings were contrary to these results and may be due to differences between *in vivo* and *in vitro* experiments, as well as experimental conditions. Our results suggest a possible mechanism by which increased arsenate uptake in STZ-induced diabetic mice was associated with PIT1 and PIT2 expression levels.

Arsenic is ubiquitous in the environment and highly toxic to all forms of the life. The arsenic metabolic cycle in mice and humans is short^[32], and its chronic toxicity is not primarily based on an accumulating concentration but rather on the functional damage of target organs over time^[33]. Diabetes is a common metabolic disease and might influence the susceptibility of many tissues to arsenic toxicity. One interesting study compared the levels of arsenic in mothers with insulin-dependent

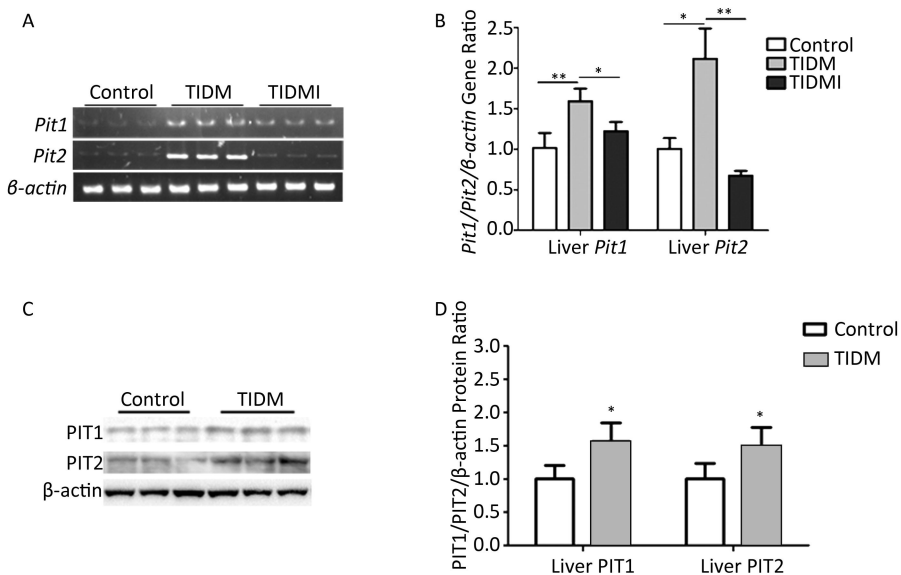


Figure 5. *Pit1*, *Pit2*, PIT1, and PIT2 expression levels in the livers of type I diabetic mellitus (T1DM) mice. (A) *Pit1* and *Pit2* mRNA expression levels were analyzed by semi-quantitative RT-PCR. (B) *Pit1* and *Pit2* mRNA expression levels were analyzed by real-time quantitative RT-PCR. (C-D) PIT1 and PIT2 protein expression levels in the liver were determined by Western blotting. The band intensity of the blot was normalized to β -actin and quantified with Image J software. Data represent means \pm SD, $n = 6$. Control, normal mice; T1DM, diabetic mice induced by STZ; T1DMI, T1DM mice treated with insulin. * $P < 0.05$, ** $P < 0.01$.

diabetes and their infants to those in mothers without diabetes and their infants. The researchers found that levels of arsenic in blood and scalp hair were significantly higher in the women with diabetes and their infants than in the women without diabetes and their infants^[34]. Recently, different effects of iAs exposure in normal and diabetic individuals were found when mice were exposed to iAs for 16 weeks. It was shown that iAs exposure had a greater influence on the metabolic profiles of diabetic mice than on that of normal mice, including amino acid metabolism, lipid metabolism, carbohydrate metabolism, and energy metabolism, especially for oxidative stress-related metabolites and metabolism^[35]. Our findings are consistent with these results, which all indicate that diabetes increases susceptibility to iAs.

In this study, we only investigated the expression of *Pit1* and *Pit2* in STZ-induced diabetic mice; other known and unknown genes associated with the uptake of arsenate have not yet been studied. Increased uptake of iAsV in the tissues of diabetic mice indicated that iAs exposure was associated with more severe damage in diabetic mice than in normal mice. Our results suggest that uptake of arsenate may be increased in diabetic patients and that arsenate may be more toxic to diabetic patients. This will be evaluated in future studies comparing differences in the uptake of arsenate between diabetic patients and normal individuals.

ABBREVIATIONS

T1DM: type I diabetes mellitus; STZ: streptozotocin; PIT1: Phosphate transporter 1, SLC20A1; PIT2: Phosphate transporter 2, SLC20A2.

CONFLICT OF INTEREST

No conflict of interest to declare.

Received: May 3, 2017;

Accepted: October 29, 2017

REFERENCES

- Villa-Belostta R, Sorribas V. Arsenate transport by sodium/phosphate cotransporter type IIb. *Toxicol Appl Pharmacol*, 2010; 247, 36-40.
- Xia Y, Wade TJ, Wu K, et al. Well water arsenic exposure, arsenic induced skin-lesions and self-reported morbidity in Inner Mongolia. *Int J Environ Res Public Health*, 2009; 6, 1107-23.
- Balakumar P, Kaur J. Arsenic exposure and cardiovascular disorders: an overview. *Cardiovasc Toxicol*, 2009; 9, 169-76.
- Tseng CH. Cardiovascular disease in arsenic-exposed subjects living in the arseniasis-hyperendemic areas in Taiwan. *Atherosclerosis*, 2008; 199, 12-8.
- Jin X, Tian X, Liu Z, et al. Maternal exposure to arsenic and cadmium and the risk of congenital heart defects in offspring. *Reprod Toxicol*, 2016; 59, 109-16.
- Quansah R, Armah FA, Essumang DK, et al. Association of arsenic with adverse pregnancy outcomes/infant mortality: a systematic review and meta-analysis. *Environ Health Perspect*, 2015; 123, 412-21.
- Aung KH, Kyi-Tha-Thu C, Sano K, et al. Prenatal Exposure to Arsenic Impairs Behavioral Flexibility and Cortical Structure in Mice. *Front Neurosci*, 2016; 10, 137.
- Kim YJ, Kim JM. Arsenic Toxicity in Male Reproduction and Development. *Dev Reprod*, 2015; 19, 167-80.
- Rosen BP. Biochemistry of arsenic detoxification. *FEBS Lett*, 2002; 529, 86-92.
- Werner A, Dehmelt L, Nalbant P. Na⁺-dependent phosphate cotransporters: the NaPi protein families. *J Exp Biol*, 1998; 201, 3135-42.
- Virkki LV, Biber J, Murer H, et al. Phosphate transporters: a tale of two solute carrier families. *Am J Physiol Renal Physiol*, 2007; 293, F643-54.
- Villa-Belostta R, Sorribas V. Role of rat sodium/phosphate cotransporters in the cell membrane transport of arsenate. *Toxicol Appl Pharmacol*, 2008; 232, 125-34.
- Reimer RJ, Edwards RH. Organic anion transport is the primary function of the SLC17/type I phosphate transporter family. *Pflugers Arch*, 2004; 447, 629-35.
- Collins JF, Bai L, Ghishan FK. The SLC20 family of proteins: dual functions as sodium-phosphate cotransporters and viral receptors. *Pflugers Arch*, 2004; 447, 647-52.
- Forster IC, Hernando N, Biber J, et al. Phosphate transporters of the SLC20 and SLC34 families. *Mol Aspects Med*, 2013; 34, 386-95.
- Villa-Belostta R, Bogaert YE, Levi M, et al. Characterization of phosphate transport in rat vascular smooth muscle cells: implications for vascular calcification. *Arterioscler Thromb Vasc Biol*, 2007; 27, 1030-6.
- Busch AE, Wagner CA, Schuster A, et al. Properties of electrogenic Pi transport by a human renal brush border Na⁺/Pi transporter. *J Am Soc Nephrol*, 1995; 6, 1547-51.
- Ravera S, Virkki LV, Murer H, et al. Deciphering PiT transport kinetics and substrate specificity using electrophysiology and flux measurements. *Am J Physiol Cell Physiol*, 2007; 293, C606-20.
- Villa-Belostta R, Sorribas V. Compensatory regulation of the sodium/phosphate cotransporters NaPi-IIc (SLC34A3) and Pit-2 (SLC20A2) during Pi deprivation and acidosis. *Pflugers Arch*, 2010; 459, 499-508.
- Ravera S, Murer H, Forster IC. An externally accessible linker region in the sodium-coupled phosphate transporter Pit-1 (SLC20A1) is important for transport function. *Cell Physiol Biochem*, 2013; 32, 187-99.

21. Atkinson MA, Eisenbarth GS. Type 1 diabetes: New perspectives on disease pathogenesis and treatment. *Lancet*, 2001; 358, 221-9.
22. Bluestone JA, Herold K, Eisenbarth G. Genetics, pathogenesis and clinical interventions in type 1 diabetes. *Nature*, 2010; 464, 1293-300.
23. Atkinson MA. The Pathogenesis and Natural History of Type 1 Diabetes. *Cold Spring Harb Perspect Med*, 2012; 2, a007641.
24. van Lunteren E, Moyer M, Spiegler S. Alterations in lung gene expression in streptozotocin-induced diabetic rats. *BMC Endocr Disord*, 2014; 14, 5.
25. Sadi G, Baloglu MC, Pektas MB. Differential gene expression in liver tissues of streptozotocin-induced diabetic rats in response to resveratrol treatment. *PLoS one*, 2015; 10, e0124968.
26. van Lunteren E, Moyer M. Gene expression profiling in the type 1 diabetes rat diaphragm. *PLoS One*, 2009; 4, e7832.
27. Jin T, Nordberg G, Sehlin J, et al. The susceptibility to nephrotoxicity of streptozotocin-induced diabetic rats subchronically exposed to cadmium chloride in drinking water. *Toxicology*, 1999; 142, 69-75.
28. Wu KK, Huan Y. Streptozotocin-Induced Diabetic Models in Mice and Rats. *Curr Protoc Pharmacol*, 2008; doi: 10.1002/0471141755.ph0547s40.
29. Fu J, Woods CG, Yehuda-Shnaidman E, et al. Low-level arsenic impairs glucose-stimulated insulin secretion in pancreatic beta cells: involvement of cellular adaptive response to oxidative stress. *Environ Health Perspect*, 2010; 118, 864-70.
30. Li H, Ren P, Onwochei M, et al. Regulation of rat Na⁺/Pi cotransporter-1 gene expression: the roles of glucose and insulin. *Am J Physiol*, 1996; 271, E1021-8.
31. Wang CC, Sorribas V, Sharma G, et al. Insulin attenuates vascular smooth muscle calcification but increases vascular smooth muscle cell phosphate transport. *Atherosclerosis*, 2007; 195, e65-75.
32. Eisler R. Arsenic hazards to humans, plants, and animals from gold mining. *Rev Environ Contam Toxicol*, 2004; 180, 133-65.
33. Hughes MF, Menache M, Thompson DJ. Dose-dependent disposition of sodium arsenate in mice following acute oral exposure. *Fundam Appl Toxicol*, 1994; 22, 80-9.
34. Kolachi NF, Kazi TG, Afridi HI, et al. Status of toxic metals in biological samples of diabetic mothers and their neonates. *Biol Trace Elem Res*, 2011; 143, 196-212.
35. Yin J, Liu S, Yu J, et al. Differential toxicity of arsenic on renal oxidative damage and urinary metabolic profiles in normal and diabetic mice. *Environ Sci Pollut Res*, 2017. doi:10.1007/s11356-017-9391-9.